Solvent-Induced Transition from Micelles in Solution to Cylindrical Microdomains in Diblock Copolymer Thin Films

Soojin Park, Jia-Yu Wang, Bokyung Kim, Wei Chen, and Thomas P. Russell*

Department of Polymer Science and Engineering, University of Massachusetts, Amherst, Massachusetts 01003

Received June 14, 2007; Revised Manuscript Received September 26, 2007

ABSTRACT: It is well-known that block copolymer thin films can be easily prepared on different substrates by spin coating. Here, we show that the cylindrical microdomains of polystyrene-*b*-poly(4-vinylpyridine) (PS-*b*-P4VP) copolymers can be oriented normal to the surface over a large area by spin coating in toluene/THF solvent mixture. The structure and size of the PS-*b*-P4VP in solution were compared with those in thin films. It was found that the cylindrical microdomains, obtained by spin coating, oriented normal to the film surface depended strongly on the amount of THF in the casting solution. The study was extended to PS-*b*-P4VP copolymers with different molecular weights and compositions, which allowed the control of the size of the cylindrical domains and the areal density of the arrays.

Introduction

Diblock copolymers, comprised of two chemically distinct chains covalently linked at one end, self-assemble into well-ordered morphologies ranging from spheres to cylinders to lamellae depending upon the volume fractions of the blocks. The immiscibility of the blocks, coupled with the connectivity of the blocks, leads to the formation of domains tens of nanometer in size, called microdomains.[1,2] The self-assembling nature of block copolymers makes them attractive candidates as templates and scaffolds for the fabrication of nanodots and nanowires[3−5] as well as for pattern transfer to the underlying substrate.[6−8] Controlling the orientation and lateral ordering of the microdomains is key to many applications. To achieve an orientation of cylindrical microdomains normal to a surface, for example, strategies have been developed to overcome preferential interactions of the blocks with the substrate, which forces an orientation of the microdomains parallel to the substrate. Several approaches have been developed, including balancing interfacial interaction,[9−13] electric fields,[14] chemically patterned substrates,[15] graphoepitaxy,[16] and epitaxial crystallization.[17] Alternatively, copolymers can be trapped in a nonequilibrium state with the desired orientation by the use of appropriate casting solvents or solvents in which the polymer swells.[18−20] Recently, a process to generate cylindrical microdomains oriented normal to a film surface by spin coating a solution of polystyrene-*b*-poly(ethyleneoxide) (PS-*b*-PEO) was reported.[19] In addition to the control of the microdomain orientation, lateral ordering of the microdomains can also be achieved by solvent annealing. Recently, arrays of hexagonally packed poly(L-lactide) (PLLA) cylindrical microdomains in a polystyrene (PS) matrix were obtained in polystyrene-*b*-poly(L-lactide) (PS-*b*-PLLA) thin films by spin-coating solutions of the copolymer in an appropriate solvent.[21]

Here, we report that by spin-coating films of polystyrene-*b*-poly(4-vinyl pyridine) (PS-*b*-P4VP) copolymer from a toluene/THF mixed solvent cylindrical microdomains oriented normal to the substrate can be achieved over a large area as illustrated in Scheme 1. Studies were performed on thin films as a function of the volume fraction of toluene in the mixed solvent by scanning force microscopy (SFM) and grazing incidence small-angle X-ray scattering (GISAXS). It was found that the morphology formed by spin coating was strongly dependent upon the solvent used due to the rate of solvent evaporation and the solubility of the blocks. Studies were performed as a function of the molecular weight of the PS-*b*-P4VP and the composition of the copolymer, which allowed control over the size of the cylindrical microdomains and the areal density of arrays.

Scheme 1. Schematic Illustration of Morphological Transition from Spherical Micelle in Solution to Cylindrical Microdomains Oriented Normal to the Film Surface after Spin Coating.

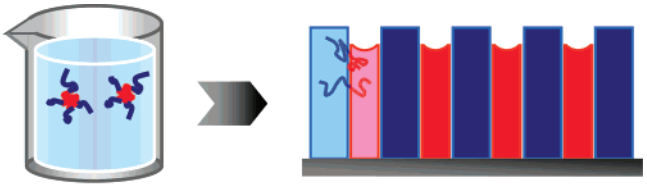

Experimental Section

Materials. Four PS-*b*-P4VP diblock copolymers (Polymer Source) were used without further purification in this experiment. The molecular weights and polydispersity are listed in Table 1. PS-*b*-P4VP copolymers were dissolved in toluene/THF mixtures having different volume ratios of toluene and THF at 70 °C for 2 h and cooled to room temperature to yield 0.5 wt % polymer solutions. PS-*b*-P4VP thin films were spin coated onto silicon substrates at 2000 rpm for 60 s.

Characterization of PS-*b*-P4VP in Solution. The molecular size of PS-*b*-P4VP in 0.5 wt % solutions was measured by dynamic light scattering (DLS). Light scattering experiments were carried out in toluene, THF, and toluene/THF solvent mixtures at 25 °C. The measurements were performed using an ALV unit equipped with an ALV/SP-125 precision goniometer (ALV-Laser Vertriebsgessellschaft m.b.H.), an Innova 70 argon laser ($\lambda_0 = 514.5$ nm, max power 3 W, Coherent) operated at 300 mW, and a photomultiplier detector (Thorn EMI Electron Tubes). All samples were systematically studied at a scattering angle of 90°. Some solutions

* To whom correspondence should be addressed. Email: russell@mail.pse.umass.edu. Phone: 413-545-2680. Fax: 413-577-1510.

10.1021/ma071321z CCC: $37.00
Published on Web 11/13/2007

Table 1. Molecular Characteristics of PS-*b*-P4VP Diblock Copolymers

sample code	PS M_n (kg/mol)	P4VP M_n (kg/mol)	M_w/M_n
S4VP69K	47.6	20.9	1.14
S4VP32K	25.0	7.0	1.07
S4VP27K	11.8	15.0	1.04
S4VP25K	19.6	5.1	1.08

were also studied at different scattering angles for static light scattering (SLS). The temperature of the sample cell was maintained within 0.1 °C at 25 °C by circulating water around the toluene bath from a bath/circulator (NESLAB, RTE-111). The polymer solutions were prefiltered several times through Millipore 0.45 μm PTFE filters. Usually, no significant loss of concentration was detected due to filtering.

Characterization of Morphology in Bulk and Thin Films. Bulk samples were prepared by drop casting 5 wt % chloroform solutions onto a Kapton film. The samples were annealed at 170 °C for 24 h after drying in air for 6 h and then left in a vacuum oven for 6 h at 50 °C and then slowly cooled to room temperature. Small angle X-ray scattering (SAXS) measurements were done under vacuum using an Osmic MaxFlux X-ray (Cu Kα, 1.54 Å) source with a Molecular Metrology camera consisting of a three-pinhole collimation system, 120 cm sample-to-detector distance (calibrated using silver behenate), and a two-dimensional, multiwire proportional detector (Molecular Metrology).

The surface topography of PS-*b*-P4VP thin films on a silicon wafer was imaged by SFM (Digital Instruments, Nanoscope III) in the tapping mode. The film thickness was measured by ellipsometry. To characterize the structure of spin-coated PS-*b*-P4VP thin films, grazing incidence small-angle X-ray scattering (GISAXS) measurements were performed at beamline X22B (National Synchrotron Light Source, Brookhaven National Laboratory) using X-rays with a wavelength of $\lambda = 1.525$ Å. The exposure time was 15 s per frame.

Results and Discussion

SAXS was used to study the microphase separation of PS-*b*-P4VP samples in bulk. Figure 1 shows the SAXS intensity as a function of scattering vector of four different molecular weight PS-*b*-P4VP samples. The scattering peak in SAXS yields the *d* spacing and microdomain structures as shown in Figure 1. The scattering profiles of S4VP69K, S4VP32K, and S4VP25K show hexagonally packed cylinders, as evidenced by the higher order scattering peaks appearing at a scattering vector of $\sqrt{3}$ times relative to the position of the first-order reflection.[2] In the case of S4VP25K copolymer, TEM was used to confirm the hexagonally packed cylinders due to the absence of the higher order reflections in the SAXS profile. The SAXS profile of S4VP27K shows scattering maxima at integral multiples of the first-order scattering peak, which indicate a lamellar microdomain morphology.[2] The scattering peak intensities of the even-order reflections are weak, since the volume fraction of S4VP27K is nearly equal.

In addition to the microphase separation in bulk, the size and structure of the PS-*b*-P4VP in solution were studied by DLS and SLS. The DLS autocorrelation functions were measured in different PS-*b*-P4VP solutions where the fractions of toluene and THF were varied. Typical results are shown in Figure 2A. The autocorrelation functions are shifted to the right (increase in the relaxation times) with increasing volume fraction of toluene. Since toluene is a good solvent for the PS block and a nonsolvent for the P4VP block, the PS-*b*-P4VP diblock copolymers form micelles with the P4VP insoluble block in the core and the PS soluble blocks in the corona. From the autocorrelation function, the hydrodynamic radius ($R_h = 39.4$ nm) of

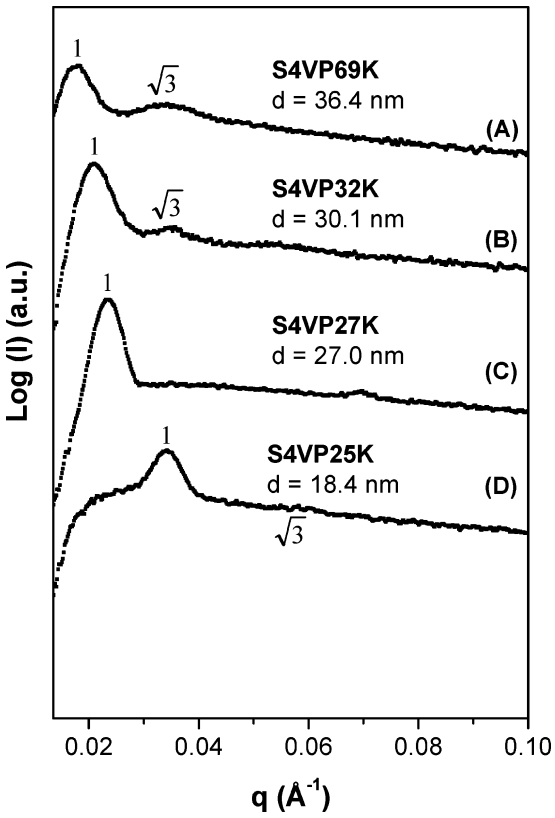

Figure 1. SAXS profiles of four different PS-*b*-P4VP samples in bulk. All samples were annealed at 170 °C for 1 day. (A) hexagonally packed cylinder, (B) hexagonally packed cylinder, (C) lamellae, and (D) hexagonally packed cylinder.

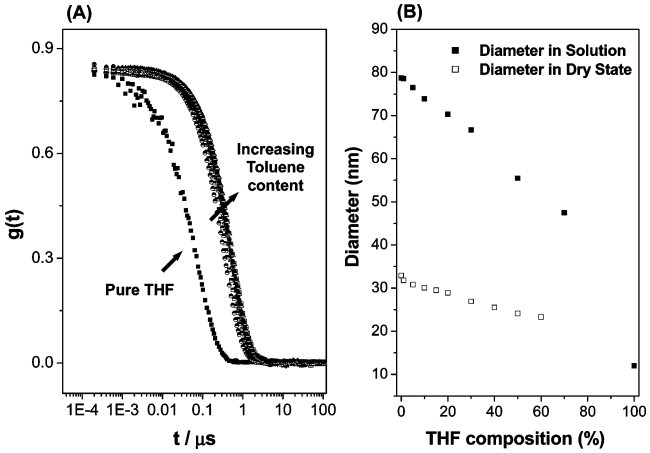

Figure 2. Hydrodynamic radius of S4VP69K measured from a variety of polymer solutions. (A) Intensity correlation functions of PS-*b*-P4VP solutions with different Toluene/THF compositions at 0.5 wt % concentrations and a scattering angle of 90°. (B) Hydrodynamic diameter in solution (closed square) and in a dry state (open square) measured from SFM.

the S4VP69K sample in pure toluene was calculated, while the radius of gyration ($R_g = 26.0$ nm) was obtained from SLS. The ratio $P = R_g/R_h$ is a sensitive fingerprint of the inner density profile. A value of $P = 26.0$ nm/39.4 nm $= 0.66$ is in the range for spherical structures ($R_g/R_h \leq 0.774$).[22] The autocorrelation functions of the other polymer solutions except for the one in pure THF are similar to that of the pure toluene solution, which means that the micelle sizes and shapes are not much different. The polydispersities of the micelles are in the range 0.01−0.03, indicating a narrow micelle size distribution for all the samples investigated. Figure 2B shows the hydrodynamic diameters of

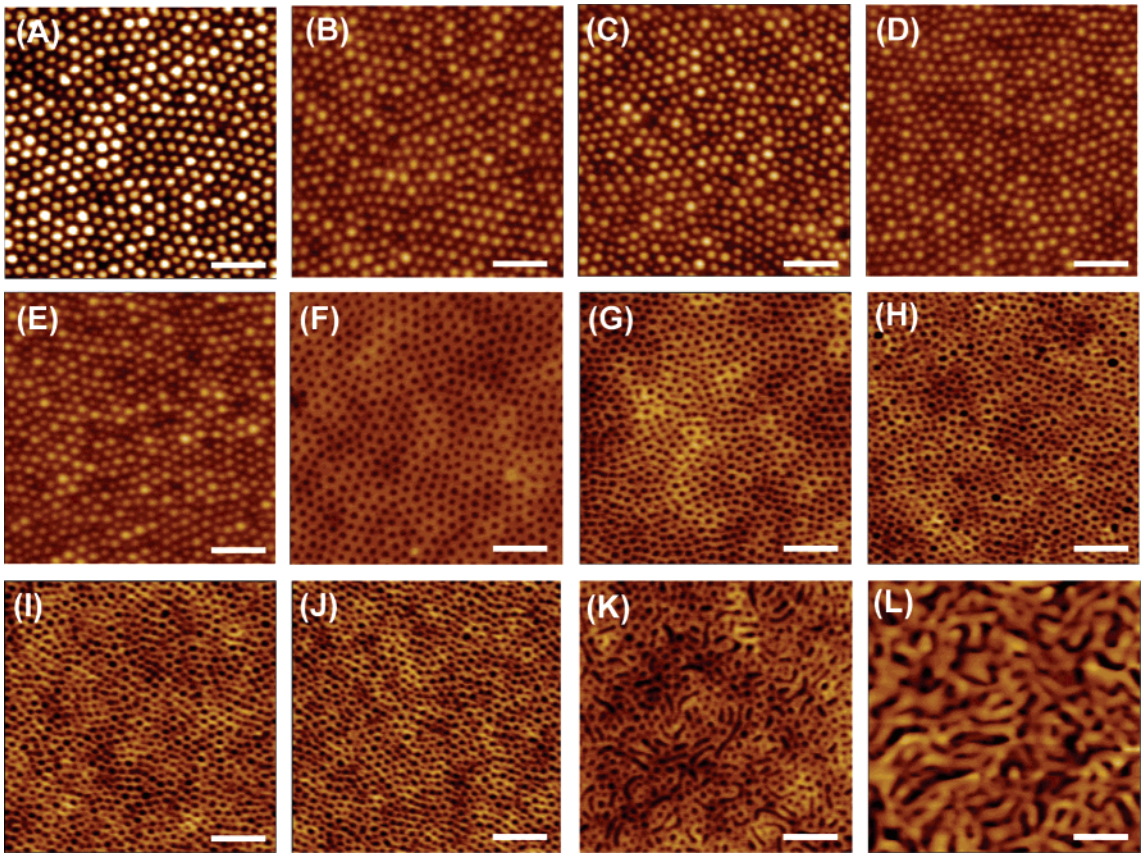

Figure 3. SFM images (height modes) of S4VP69K (47.6−20.9 k) developed in different casting solutions: (A) pure toluene, (B) toluene/THF = 99/1, (C) toluene/THF = 95/5, (D) toluene/THF = 90/10, (E) toluene/THF = 85/15, (F) toluene/THF = 80/20, (G) toluene/THF = 70/30, (H) toluene/THF = 60/40, (I) toluene/THF = 50/50, (J) toluene/THF = 40/60, (K) toluene/THF = 30/70, and (L) pure THF. All solvent compositions are expressed in volume percentage (v/v). Scale bar is 200 nm.

nine different PS-*b*-P4VP solutions calculated from the autocorrelation function in Figure 2A. When the volume fraction of THF increases, the size of micelles gradually decreased except for that in pure THF. For the pure THF solution, the autocorrelation function is far from those of other polymer solutions. The R_h value of THF polymer solution is 6.0 nm, which is consistent with the size of a random coil of PS of the same molecular weight.[23] It is interesting to note that the micelle size decreases with increasing THF composition; this is because THF is a less selective solvent for PS than toluene. The micelle size in solution is about 2 times larger than the size of the structures seen in films, as shown in Figure 2B. The two different sizes can be explained by the presence of solvent; the corona of the micelles in solution is in contact with the solvent and is, therefore, swollen and hence the larger size.

To compare the structure or aggregation of PS-*b*-P4VP in solution with the structure seen in thin films, the films were spin coated at 2000 rpm from 0.5 wt % solutions of PS-*b*-P4VP in toluene, THF, and toluene/THF mixture onto silicon wafers. Figure 3 shows the morphologies in thin films obtained from 12 different S4VP69K polymer solutions where the concentration of the toluene/THF mixtures ranged from pure toluene to pure THF. All samples were dried in vacuum overnight at 30 °C before SFM measurements. The film thickness of the PS-*b*-P4VP casting from pure toluene solution was 23.5 nm while that from pure THF solution was 24.5 nm. It should be noted that there is only 1 nm thickness difference between the two extreme conditions. Dimple-type structures (dried micelles) were observed from polymer solutions in THF/toluene (15/85 v/v) mixtures as shown in Figure 3A−E. However, when the concentration of the solvent was changed to 20/80, only a 5% increase in THF, a transformation of morphology from dimple-type structure to cylinders oriented normal to the surface occurred. Figure 3F shows a thin film morphology consisting of arrays of hexagonally packed P4VP microdomains oriented normal to the surface in a PS matrix. The SFM image measured in the phase mode shows the harder material, the P4VP blocks, as brighter color, while the PS matrix is dark (see Supporting Information, Figure S1). After the film was floated on a HF buffer (5 wt %) solution, it was transferred onto a silicon wafer so that both the top and the bottom of the film could be examined. Both the top and the bottom of the film showed a hexagonal array of cylindrical microdomains, indicating that the microdomains spanned the entire film (see Supporting Information, Figure S1).

Increasing the THF content in the solvent mixture to 60% shows a similar morphology, though the size of the microdomains had decreased. In polymer solutions containing 70% THF, cylindrical microdomains oriented both normal to and parallel to the surface were seen as shown in Figure 3K. In pure THF, a wormlike morphology was seen.

The orientation of the microdomains normal to the surface can be attributed to the solvent evaporation and the solubility of the constituted blocks. With toluene and THF, the selectivity of the solvent for PS-*b*-P4VP can be described by the equation $\chi = \chi_H + \chi_S = V_i(\delta_i - \delta_j)^2/RT + 0.34$, where V is the molar volume and δ is the solubility parameter for solvent i and polymer j.[24] The solubility parameters of PS and P4VP are 18.6 $(MPa)^{0.5}$ and 22.2 $(MPa)^{0.5}$, respectively.[25] For a polymer to be soluble in a solvent at a particular temperature, χ must be below 0.5 even at high levels of polymer concentration in solution. On the basis of this evaluation, toluene and THF are defined as

Table 2. The Selectivity and Vapor Pressure of Solvents

solvent	molar vol (cm^3/mol)	$\chi_{PS-solvent}$	$\chi_{P4VP-solvent}$	$\delta_{solvnet}$ $(MPa)^{0.5}$	vp (mmHg)
toluene	106.9	0.37	1.03	18.2	28.5
THF	81.7	0.35	0.6	19.4	176

being PS selective solvents, since $\chi_{PS-solvent} < 0.5$ and $\chi_{P4VP-solvent} > 0.5$. From the calculation of interaction parameters, we can conclude that toluene is a more selective solvent for PS than THF. Details of the selectivity and the vapor pressure for the solvents are listed in Table 2. PS selective solvents having two different vapor pressures at ambient temperature were used for spin coating. We observed the morphological transition from a dimple type to cylindrical microdomains with increasing THF concentration or as the solvent became less selective for PS. In addition, the evaporation of THF is faster than toluene. Consequently, the combination of these two (selectivity and evaporation rate) has induced the transformation in the morphology to cylindrical microdomains oriented normal to the film surface. In addition, the solvent imparts substantial mobility to the copolymer which enhances lateral order. The morphologies obtained upon evaporation of the solvent are, of course, trapped in a nonequilibrium state, and heating the film above the T_g's of the microdomains will lead to films having cylindrical microdomains oriented parallel to the surface.[18,19,21]

We extended this idea to other PS-*b*-P4VP samples having different molecular weights and volume fractions of components. Figure 4 shows the SFM images of these samples after spin coating and solvent annealing in toluene/THF solvent mixtures. When PS-*b*-P4VP copolymers were spin coated from a toluene/THF (80/20 v/v) solvent mixture onto silicon substrate, the microdomains of all thin films were oriented normal to the film surface, as shown in Figure 4. The films were exposed to toluene/THF mixture (20/80) vapor for 12 h to induce mobility and allow microphase separation to occur under N_2. To control the solvent vapor treatment process, the samples were kept at a constant temperature (23 °C) in a small vessel having solvent bubbling equipment. After solvent annealing, highly oriented PS-*b*-P4VP cylinders can be obtained without any significant changes in the size of the microdomains, as shown in Figure 4D−F. In contrast to the microdomain size in bulk, the center-to-center distance (34.0 ± 1.8 nm) of S4VP27K film is larger than that of S4VP32K (32.8 ± 1.4 nm), since the micelle size in solution depends upon the molecular weight of the P4VP blocks.[22] In the inset of Figure 4D−F, the separation distance between cylindrical microdomains was compared. It should be noted that the size of the microdomains obtained in spin-coated films is strongly affected by the size of the micelles in polymer solution and cylindrical microdomains are obtained immediately after spin coating.

GISAXS was used to investigate the morphology of the PS-*b*-P4VP and the orientation within the samples, as shown in Figure 4D−F. Figure 5 shows the GISAXS patterns measured above the critical angle ($\alpha = 0.18°$) of polymer ($\alpha_c = 0.16°$). When the incidence angle was set above the critical angle of the polymer (0.16°) but below the critical angle for Si (0.22°), it allowed the X-rays to penetrate through the polymer film and to be totally reflected at the Si interface thereby enhancing the scattering from the polymer film in comparison to measurements done below the critical angle of the polymer. Figure 5A−C shows GISAXS characteristics of PS-*b*-P4VP cylindrical microdomains highly oriented normal to the film surface as evidenced by the extension of the scattering along q_z direction. This "Bragg rod" scattering arises from a truncation of the cylindrical domains at the surface. In the intensity of scattering

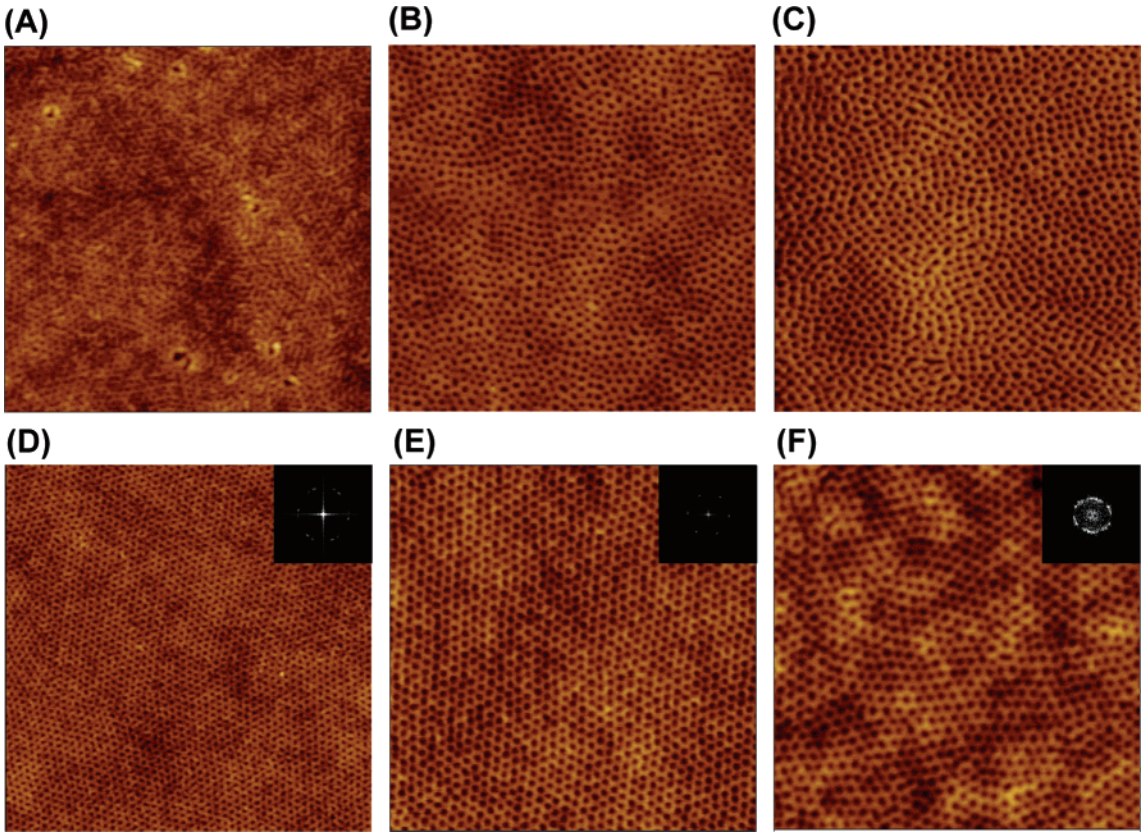

Figure 4. SFM images of as-spun (A−C) and solvent annealed (D−F) PS-*b*-P4VP films with different molecular weights and volume fractions (height mode, 1 μm × 1 μm). (A,D) S4VP25K, (B,E) S4VP32K, and (C,F) S4VP27K. The cylindrical microdomains of all thin films are oriented normal to the film surface.

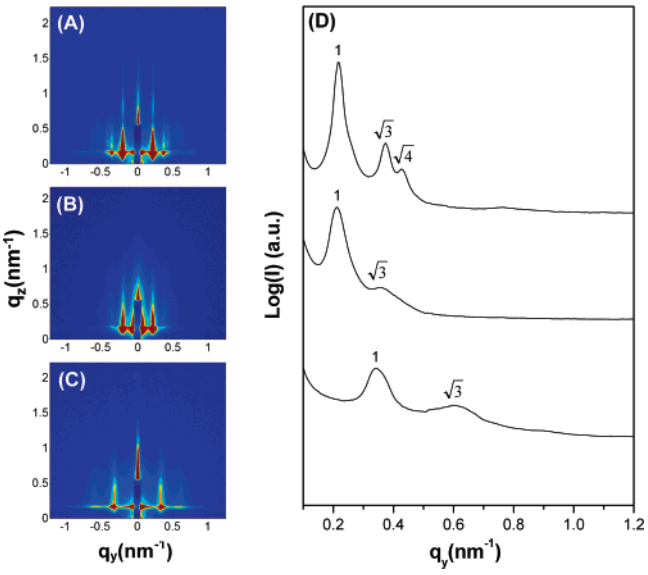

Figure 5. GISAXS patterns of three different PS-*b*-P4VP thin films: (A) S4VP32K, (B) S4VP27K, and (C) S4VP25K. (D) Intensity of scattering as a function of q_y of the GISAXS patterns in the left-hand side. GISAXS patterns show the structure of highly oriented PS-*b*-P4VP cylindrical microdomains with perpendicular orientation as evidenced by the extension of the scattering along q_z direction.

as a function of q_y, the characteristic in-plane density variation is shown in Figure 5D. The values of q_y corresponding to the peak positions are characteristic of hexagonally packed cylindrical microdomains. In addition, the center-to-center distance between the cylindrical microdomains for S4VP27K (*d* spacing, 29.5 nm) sample is larger than that of S4VP32K (*d* spacing, 29.0 nm), which is consistent with the SFM results shown in Figure 4.

Conclusions

We have shown that PS-*b*-P4VP thin films form cylindrical microdomains oriented normal to the film surface during spin coating from toluene/THF solvent mixtures due to solvent selectivity and evaporation rate. The orientation is observed to be independent of the PS-*b*-P4VP molecular weights and volume fractions of the blocks. After solvent annealing, highly ordered PS-*b*-P4VP cylinders can be obtained without significant changes in size and center-to-center distances of the microdomains. Since the cylindrical microdomains oriented normal to the film surface can be made into a nanoporous structure via surface reconstruction,[26] a simple, rapid route for the generation of nanoporous templates for the fabrication of nanostructured materials or for pattern transfer has been demonstrated.

Acknowledgment. This work was supported by the NSF-supported Materials Research Science and Engineering Center (DMR-0213695) and Center for Hierarchical Manufacturing (DMI-0531171) at the University of Massachusetts, Amherst, and the U.S. Department of Energy, Office of Basic Energy Sciences (DE-FG02-96ER45612). S.P. was supported by the Korea Research Foundation Grant funded by the Korean Government (KRF-2006-214-D00047). We thank Dr. B. M. Ocko for assistance with the GISAXS on beamline X22B at the National Synchrotron Light Source, Brookhaven National laboratory, which is supported by the US Department of Energy, Basic Energy Sciences (DE-AC02-98CH10886). We also thank D. A. Hoagland and J. Harner for assistance with the LS measurements.

Supporting Information Available: SFM images of as-spun S4VP69K. This material is available free of charge via the Internet at http://pubs.acs.org.

References and Notes

(1) Bates, F. S.; Fredrickson, G. H. *Annu. Rev. Phys. Chem.* **1990**, *41*, 525.
(2) Hamley, I. W. *The Physics of Block Copolymers*; Oxford University Press: New York, 1998.
(3) Thurn-Albrecht, T.; Schotter, J.; Kästle, G. A.; Emley, N.; Shibauchi, T.; Krusin-Elbaum, L.; Guarini, K.; Black, C. T.; Tuominen, M. T.; Russell, T. P. *Science* **2000**, *290*, 2126−2129.
(4) Spatz, J. P.; Chan, V. Z.-H.; Mößmer, S.; Kamm, F.-M.; Plettl, A.; Ziemann, P.; Möller, M. *Adv. Mater.* **2002**, *14*, 1827−1832.
(5) Fan, H. J.; Werner, P.; Zacharias, M. *Small.* **2006**, *2*, 700−717.
(6) Park, M.; Harrison, C.; Chaikin, P. M.; Register, R. A.; Adamson, D. H. *Science* **1997**, *276*, 1401−1404.
(7) Fasolka, M. J.; Mayes, A. M. *Annu. Rev. Mater. Res.* **2001**, *31*, 323−355.
(8) Segalman, R. A. *Mater. Sci. Eng., R* **2005**, *48*, 191−226.
(9) Mansky, P.; Liu, Y.; Huang, E.; Russell, T. P.; Hawker, C. J. *Science* **1997**, *275*, 1458−1460.
(10) Hawker, C. J.; Russell, T. P. *MRS Bull.* **2005**, *30*, 952−966.
(11) Yang, X.; Xiao, S.; Liu, C.; Phlhos, K.; Minor, K. *J. Vac. Sci. Technol., B: Microelectron.* **2004**, *22*, 3331−3334.
(12) In, I.; La, Y.-H.; Park, S.-M.; Nealey, P. F.; Gopalan, P. *Langmuir* **2006**, *22*, 7855−7860.
(13) Xu, T.; Kim, H.-C.; DeRouchey, J.; Seney, C.; Levesque, C.; Martin, P.; Stafford, C. M.; Russell, T. P. *Polymer* **2001**, *42*, 9091−9095.
(14) Thurn-Albrecht, T.; DeRouchey, J.; Russell, T. P. *Macromolecules* **2000**, *33*, 3250−3253.
(15) Stoykovich, M. P.; Müller, M.; Kim, S. O.; Solak, H. H.; Edwards, E. W.; de Pablo, J. J.; Nealey, P. F. *Science* **2005**, *308*, 1442−1446.
(16) Segalman, R. A.; Yokoyama, H.; Kramer, E. J. *Adv. Mater.* **2001**, *13*, 1152−1155.
(17) De Rosa, C.; Park, C.; Thomas, E. L.; Lotz, B. *Nature* **2000**, *405*, 433−437.
(18) Kim, G.; Libera, M. *Macromolecules* **1998**, *31*, 2569−2577.
(19) Kim, S. H.; Misner, M. J.; Xu, T.; Kimura, M.; Russell, T. P. *Adv. Mater.* **2004**, *16*, 226−231.
(20) Sidorenko, A.; Tokarev, I.; Minko, S.; Stamm, M. *J. Am. Chem. Soc.* **2003**, *125*, 12211−12216.
(21) Ho, R.-M.; Tseng, W.-H.; Fan, H.-W.; Chiang, Y.-W.; Lin, C.-C.; Ko, B.-T.; Huang, B.-H. *Polymer* **2005**, *46*, 9362−9377.
(22) Antonietti, M.; Heinz, S.; Schmidt, M.; Rosenauer, C. *Macromolecules* **1994**, *27*, 3276−3281.
(23) Park, S.; Chang, T.; Park, I. H. *Macromolecules* **1991**, *24*, 5729−5731.
(24) Mark, J. E. *Physical properties of polymers handbook*; AIP Press: New York, 1996.
(25) Brandrup, J.; Immergut, E. H.; Grulke, E. A.; Abe, A.; Bloch, D. R. *Polymer Handbook, 4th ed.*; Wiley: New York, 1999.
(26) Xu, T.; Stevens, J.; Villa, J.; Goldbach, J. T.; Guarini, K. W.; Black, C. T.; Hawker, C. J.; Russell, T. P. *Adv. Funct. Mater.* **2003**, *13*, 698−702.

MA071321Z